Acta Crystallographica Section F
Structural Biology and Crystallization Communications
ISSN 1744-3091

Overexpression, purification, crystallization and preliminary X-ray analysis of Rv2780 from *Mycobacterium tuberculosis* H37Rv

Sarvind Mani Tripathi and Ravishankar Ramachandran*

Molecular and Structural Biology Division, Central Drug Research Institute, PO Box 173, Chattar Manzil, Mahatma Gandhi Marg, Lucknow 226001, India

Correspondence e-mail: r_ravishankar@cdri.res.in

Received 16 February 2008
Accepted 20 March 2008

Rv2780, an alanine dehydrogenase from *Mycobacterium tuberculosis* (MtAlaDH), catalyzes the NAD-dependent interconversion of alanine and pyruvate. Alanine dehydrogenase is released into the culture medium in substantial amounts by virulent strains of mycobacteria and is not found in the vaccine strain of tuberculosis. Crystals of recombinant MtAlaDH were grown from 2 *M* ammonium sulfate solution at ∼12 mg ml^{-1} protein concentration in two crystal forms which occur in the presence and absence of NAD/pyruvate, respectively. Diffraction data extending to 2.6 Å were collected at room temperature from both apo and ternary complex crystals. Crystals of the apoenzyme have unit-cell parameters $a = 173.89$, $b = 127.07$, $c = 135.95$ Å. They are rod-like in shape and belong to space group $C2$. They contain a hexamer in the asymmetric unit. Crystals of the ternary complex belong to space group $P4_32_12$ and have unit-cell parameters $a = b = 88.99$, $c = 373.85$ Å. There are three subunits in the asymmetric unit of the holoenzyme crystals.

1. Introduction

Mycobacterium tuberculosis exhibits significant changes in gene expression during the latent/persistent stage of infection. Proteomic analysis of nutrient-starved/latent-phase bacteria suggested decreased expression of proteins involved in energy metabolism, lipid biosynthesis and cell division in addition to induction of stringent response and several other genes that may play a role in long-term survival within the host (Betts *et al.*, 2002; Stewart *et al.*, 2003). L-Alanine dehydrogenase, which is encoded by *ald*, catalyzes the oxidative deamination of L-alanine or, in the reverse reaction, the reductive amination of pyruvate. This enzyme is known to be required for normal sporulation in *Bacillius subtilis* (Siranosian *et al.*, 1993) and for normal development of *Myxococcus xanthus* (Ward *et al.*, 2000). In mycobacteria, L-alanine dehydrogenase is a secretory antigen that is associated with bacterial persistence during infection. Expression of *ald* is upregulated in *M. tuberculosis* upon nutrient starvation and in *M. marinum* during persistence within the granulomas of infected frogs (Chan *et al.*, 2002). L-Alanine dehydrogenase production and activity was also increased when *M. tuberculosis* and *M. smegmatis* were shifted from aerobic to anaerobic growth conditions (Rosenkrands *et al.*, 2002; Usha *et al.*, 2002). The enzyme was rated among the top three targets against persistence in an analysis by Hasan *et al.* (2006). Western blotting has failed to detect L-alanine dehydrogenase in the BCG (Bacille Calmette-Guérin) strain, even though the *ald* gene has been identified by DNA hybridization; this absence of functional protein arises from a single-nucleotide deletion within the *ald* gene that causes a frame-shift mutation and disrupts the full-length protein.

The overall reaction catalysed by Ald is

$$\text{L-Alanine} + \text{NAD}^+ + \text{H}_2\text{O} \longleftrightarrow \text{pyruvate} + \text{NADH} + \text{H}^+ + \text{NH}_4^+.$$

L-Alanine dehydrogenases purified from sources such as *M. tuberculosis* (Andersen *et al.*, 1992), *Bacillus* spp. (Ohshima *et al.*, 1990), *Phormidium lapideum* (Sawa *et al.*, 1994) and *Streptomyces phaeo-*

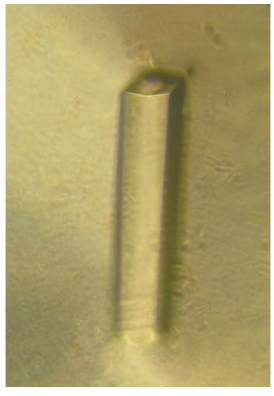

chromogenes (Itoh & Morikawa, 1983) exist as homohexamers, with a subunit molecular weight of ∼40 000 Da, while octameric and tetrameric oligomeric associations have been reported for the enzymes from *S. aureofaciens* (Vancurova *et al.*, 1989) and *S. fradiae* (Vancura *et al.*, 1989), respectively. The crystal structures of alanine dehydrogenase from *P. lapideum* (cyanobacteria; Baker *et al.*, 1998) and *Archaeoglobus fulgidis* (hyperthermophilic archea; Gallagher *et al.*, 2004) have been reported. The level of sequence similarity between Ald from *P. lapideum* and those from other eubacteria is high. These enzymes are comprised of a C-terminal NAD-binding Rossmann-fold domain and a catalytic domain. The domains are separated by a cleft. However, bacterial ALDs exhibit lower homology in sequence and in structure compared with other amino-acid dehydrogenases including phenylalanine dehydrogenase (Vanhooke *et al.*, 1999), leucine dehydrogenase (Baker *et al.*, 1995) and glutamate dehydrogenase (Stillman *et al.*, 1993).

Owing to the implied importance of Ald in the virulence of *M. tuberculosis*, we have cloned, expressed, purified and crystallized the *M. tuberculosis* protein (MtAlaDH). The structure of the apoenzyme has been solved using molecular replacement and reveals a hexamer in the asymmetric unit of the crystal. Similar calculations show that there are three subunits in the asymmetric unit of the crystals of the holoenzyme. The structures are expected to be a valuable tool in identifying novel inhibitors using structure-based strategies.

2. Experimental methods

2.1. Protein expression and purification

The *ald* gene (*Rv2780*) was amplified from *M. tuberculosis* H37Rv genomic DNA using the following primers: the sense primer 5′-ATGCGCT**AGCATG**CGCGTCGGTATTTCCG-3′ and the anti-sense primer 5′-TATA**AAGCTT**GGCCAGCACGCTGG-3′ containing *Nhe*I and *Hin*dIII restriction sites (nucleotides shown in bold). The amplified PCR product was digested with *Nhe*I and *Hin*dIII and ligated into pET23a (Novagen) vector digested with the same enzyme. This attaches a tag comprising ACGRTRAHHHHHH at the C-terminal end and allows purification using affinity chromatography. Clones were screened by restriction digestion and the resulting construct was transformed into *Escherichia coli* C41 (DE3). The integrity of the insert was verified by sequencing.

A single colony was inoculated into 50 ml YT medium containing 50 µg ml^{-1} ampicillin and grown overnight at 310 K. These cells were used to inoculate 1 l YT medium containing 50 µg ml^{-1} ampicillin and expression was induced with 0.2 m*M* isopropyl *β*-D-1-thio-galactopyranoside (IPTG) at an optical density of 0.6 at 600 nm. Cells were grown at 303 K for 6 h after induction with IPTG. The IPTG-induced cells were harvested, resuspended in ice-cold 50 m*M* Tris–HCl pH 7.2, 300 m*M* NaCl, 10 m*M* imidazole (buffer *A*) and sonicated. The crude lysate was centrifuged at 27 000*g* for 30 min. The supernatant was applied onto a Ni–IDA column pre-equilibrated with buffer *A*. The protein was eluted using the same buffer supplemented with 500 m*M* imidazole. Fractions containing the protein were pooled and precipitated by ammonium sulfate (60%) saturation. The pellet was resuspended in 50 m*M* Tris–HCl pH 7.2, 50 m*M* NaCl, 5 m*M* EDTA, 2 m*M* *β*-mercaptoethanol (buffer *B*) and further purified on a Superdex S-200 (Amersham Biosciences) gel-filtration column equilibrated with buffer *B*. The protein was pooled and concentrated to 12 mg ml^{-1} using a 30 kDa cutoff Centricon (Amicon). The purified protein with a hexahistidine tag at the C-terminus was assayed for activity and protein concentrations were determined with the Bradford reagent (Bradford, 1976) using bovine serum albumin as a standard. MtAlaDH remained stable at 277 K without degradation for up to one week. The purity of the protein was confirmed using 12% SDS–PAGE (Fig. 1). Photometric determination of enzyme activity was accomplished by measuring the rate of the production of NADH at 340 nm that accompanies the conversion of alanine into pyruvate in the oxidative deamination.

2.2. Crystallization

MtAlaDH was concentrated to ∼12 mg ml^{-1} in a buffer comprising 50 m*M* Tris pH 7.2, 50 m*M* NaCl, 5 m*M* EDTA and 2 m*M* *β*-mercaptoethanol. All crystallization experiments were carried out by the hanging-drop vapour-diffusion method in 24-well Linbro tissue-culture plates (ICN Inc.). The experiments were set up exploiting two different sparse-matrix screening strategies (Mazeed *et al.*, 2003; Jancarik & Kim, 1991; Cudney *et al.*, 1994). Each hanging drop was prepared using 2 µl protein sample and 1 µl reservoir solution and was equilibrated against 500 µl reservoir solution. The apo and ternary complex crystals were obtained under similar crystallization conditions, except that 5 m*M* NAD and 10 m*M* pyruvate were added to the crystallization solution in the case of the ternary complex crystals. Good diffraction-quality crystals of MtAlaDH were obtained from a reservoir solution consisting of 2 *M* ammonium sulfate. Single rod-shaped crystals corresponding to the apo form

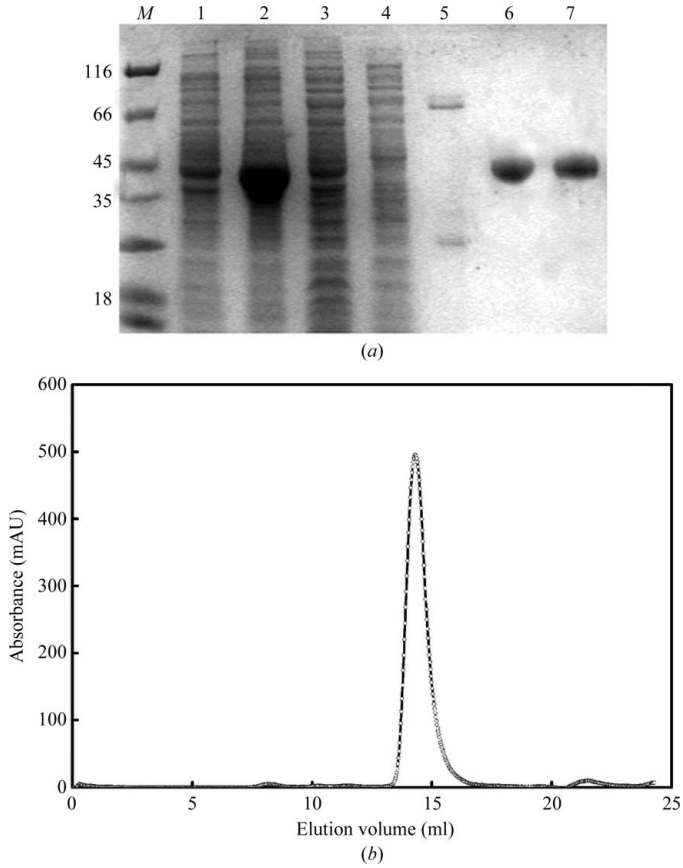

Figure 1
(*a*) Purification of MtAlaDH. Lane *M*, molecular-weight markers; lane 1, uninduced cell lysate; lane 2, cell lysate induced with 0.5 m*M* IPTG; lane 3, supernatant; lane 4, sample washed with 10 m*M* imidazole; lane 5, sample washed with 80 m*M* imidazole; lane 6, purified protein after Ni–IDA; lane 7, purified protein after size-exclusion chromatography. (*b*) Gel-filtration profile of MtAlaDH. Protein eluted at 12.56 ml, corresponding to a hexameric association of the subunits.

(Fig. 2) grew to typical dimensions of 1.4 × 0.7 × 0.4 mm. In the case of the ternary complex, large diamond-shaped crystals started appearing within 3–4 d and grew to typical maximum dimensions of 1.7 × 1 × 0.7 mm.

2.3. Data collection and processing

A single crystal was mounted in a capillary for both the apo protein and the complex with NAD and pyruvate. Diffraction data were collected using a MAR-DTB image-plate detector and a Rigaku Micromax-007 X-ray generator coupled with Varimax-HR optics. Crystal-to-detector distances of 200 and 240 mm were used for the apo and ternary crystal forms, respectively, and exposure times of 60 and 10 s per frame were used in the respective data collections. An oscillation range of 1° was used for the apoenzyme crystals. One cell edge of the ternary complex crystals was large; the oscillation range was therefore reduced to 0.5° and the data could be processed successfully. The resolution of the larger cell edge was possible with the use of the Rigaku instrument and associated optics, which allow resolution of cell edges typically up to 450 Å. Although the holoenzyme crystals diffract to better than 2.6 Å resolution (Fig. 3), the geometry and limitations of the home source only allowed data collection to this resolution. Diffraction images were indexed, integrated and scaled using the *HKL*-2000 package (Otwinowski & Minor, 1997). The crystals of the apoenzyme were monoclinic, with unit-cell parameters $a = 173.9$, $b = 127.1$, $c = 135.9$ Å, and belonged to space group $C2$. The ternary complex crystallized in space group $P4_32_12$, with unit-cell parameters $a = b = 88.99$, $c = 373.85$ Å. Both crystal forms diffracted to 2.6 Å and the statistics are summarized in Table 1.

2.4. Structure solution

The crystals of the apoenzyme were phased by the molecular-replacement approach using *AMoRe* (Navaza, 1994) as implemented in the *CCP*4 package (Collaborative Computational Project, Number 4, 1994). Sequence alignment with known structures in the PDB showed that the alanine dehydrogenase from *P. lapideum* (Baker *et al.*, 1998; PDB code 1pjb) has nearly 45% sequence similarity. A search model for molecular-replacement calculations was generated from 1pjb in which non-identical amino acids were replaced by alanine. A clear solution was obtained with a correlation coefficient of 56.2% and an R factor of 47.8% using data in the resolution range 15–3 Å. The solution exhibits good packing with no steric hindrances. The asymmetric unit contains a hexamer, which corresponds to a Matthews coefficient (Matthews, 1968) of 2.8 Å^3 Da^{-1} and a solvent content of 56.3%. Our previous experiments involving size-exclusion chromatography were consistent with a hexameric association in MtAlaDH. The initial molecular-replacement calculations and maps in the case of the holoenzyme reveal clear density for the NAD and pyruvate moieties, confirming the occurrence of the ternary complex in the crystal. The presence of NAD in the dissolved crystals was also spectroscopically confirmed. There are three subunits in the asymmetric unit, corresponding to a solvent content of about 59.8%. Phase

Table 1
Data-collection statistics for crystals of the apoprotein and the ternary complex with NAD/pyruvate.

Values in parentheses are for the highest resolution shell.

	Apo enzyme	Ternary complex
Wavelength (Å)	1.5418	1.5418
Space group	$C2$	$P4_32_12$
Unit-cell parameters (Å)	$a = 173.89$, $b = 127.07$, $c = 135.95$	$a = 88.99$, $b = 88.99$, $c = 373.85$
Resolution range (Å)	24.56–2.6 (2.7–2.6)	41.92–2.6 (2.7–2.6)
No. of measured reflections	79674 (6960)	46693 (4621)
No. of unique reflections	46867 (3026)	6670 (783)
Multiplicity	1.7 (2.3)	7.0 (5.9)
$\langle I/\sigma(I)\rangle$	9.6 (1.6)	30.3 (7.9)
Completeness (%)	97.6 (85.5)	98.0 (99.2)
$R_{\rm merge}$†	0.11 (0.46)	0.07 (0.24)

† $R_{\rm merge} = \sum_{hkl}\sum_i |I_i(hkl) - \langle I(hkl)\rangle| / \sum_{hkl}\sum_i I_i(hkl)$, where $I_i(hkl)$ is the ith measurement of reflection hkl and $\langle I(hkl)\rangle$ is the average value of the reflection intensity.

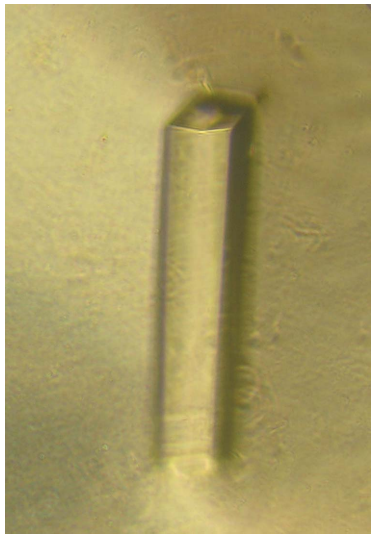

Figure 2
Crystal of apo Rv2780 (MtAlaDH). The crystals have approximate dimensions of 1.4 × 0.7 × 0.4 mm.

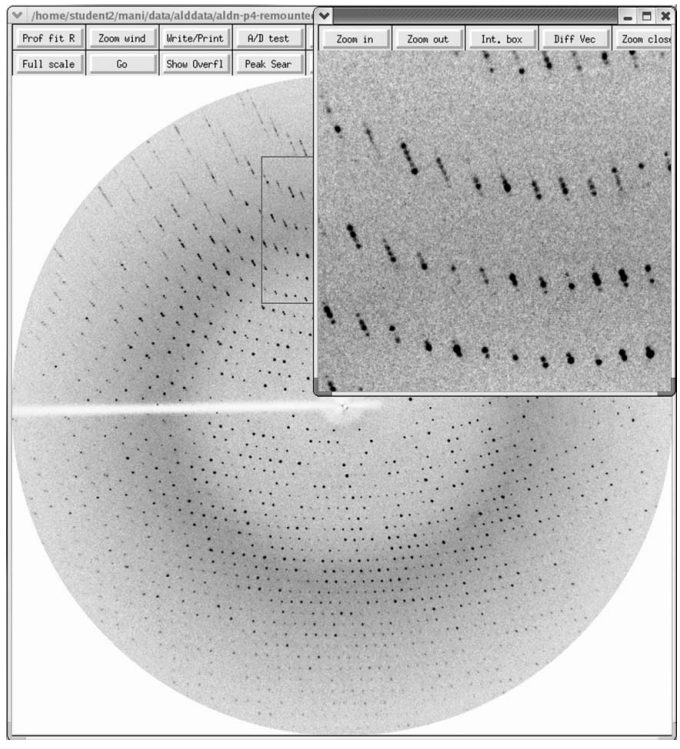

Figure 3
Snapshot of the diffraction pattern of the ternary complex crystals. The image corresponds to a 0.5 ° oscillation with 10 s exposure time and a crystal-to-detector distance of 240 mm. The edge of the circle corresponds to 2.6 Å.

improvement and model building of the structures are presently in progress.

Note added in proof: After submission of the manuscript, we were alerted that structures of the apo and holo forms of the enzyme had been published in the meantime by another group (Agren *et al.*, 2008). The crystal forms described differ from those reported here.

This work was supported by a Council of Scientific and Industrial Research, India (CSIR) network grant NWP0038 (formerly SMM003). Computational support was from CSIR grant CMM0017. We thank Dr Amit Sharma (International Centre for Genetic Engineering and Biotechnology, New Delhi, India) for use of the Rigaku Micromax-007 X-ray generator. SMT is a senior research fellow of the University Grants Commission, India. This is communication No. 7472 from CDRI.

References

Agren, D., Stehr, M., Berthold, C. L., Kapoor, S., Oehlmann, W., Singh, M. & Schneider, G. (2008). *J. Mol. Biol.* **377**, 1161–1173.
Andersen, A. B., Andersen, P. & Ljungqvist, L. (1992). *Infect. Immun.* **60**, 2317–2323.
Baker, P. J., Sawa, Y., Shibata, H., Sedelnikova, S. E. & Rice, D. W. (1998). *Nature Struct. Biol.* **5**, 561–567.
Baker, P. J., Turnbull, A. P., Sedelnikova, S. E., Stillman, T. J. & Rice, D. W. (1995). *Structure*, **3**, 693–705.
Betts, J. C., Lukey, P. T., Robb, L. C., McAdam, R. A. & Duncan, K. (2002). *Mol. Microbiol.* **43**, 717–731.
Bradford, M. M. (1976). *Anal. Biochem.* **72**, 248–254.
Chan, K., Knaak, T., Satkamp, L., Humbert, O., Falkow, S. & Ramakrishnan, L. (2002). *Proc. Natl Acad. Sci. USA*, **99**, 3920–3925.
Collaborative Computational Project, Number 4 (1994). *Acta Cryst.* D**50**, 760–763.
Cudney, R., Patel, S., Weisgraber, K., Newhouse, Y. & McPherson, A. (1994). *Acta Cryst.* D**50**, 414–423.
Gallagher, D. T., Monbouquette, H. G., Schroder, I., Robinson, H., Holden, M. J. & Smith, N. N. (2004). *J. Mol. Biol.* **342**, 119–130.
Hasan, S., Daugelat, S., Srinivasa Rao, P. S. & Schreiber, M. (2006). *PLOS Comput. Biol.* **2**, e61.
Itoh, N. & Morikawa, R. (1983). *Agric. Biol. Chem.* **47**, 2511–2519.
Jancarik, J. & Kim, S.-H. (1991). *J. Appl. Cryst.* **24**, 409–411.
Matthews, B. W. (1968). *J. Mol. Biol.* **33**, 491–497.
Mazeed, S., Ofek, G., Belachew, A., Huang, C. C., Zhou, T. & Kwong, P. D. (2003). *Structure*, **11**, 1061–1070.
Navaza, J. (1994). *Acta Cryst.* A**50**, 157–163.
Ohshima, T., Sakane, M., Yamazaki, T. & Soda, K. (1990). *Eur. J. Biochem.* **191**, 715–720.
Otwinowski, Z. & Minor, W. (1997). *Methods Enzymol.* **276**, 307–326.
Rosenkrands, I., Slayden, R. A., Crawford, J., Aagaard, C., Barry, C. E. III & Andersen, P. (2002). *J. Bacteriol.* **184**, 3485–3491.
Sawa, Y., Tani, M., Murata, K., Shibata, H. & Ochiai, H. (1994). *J. Biochem.* **116**, 995–1000.
Siranosian, K. J., Ireton, K. & Grossman, A. D. (1993). *J. Bacteriol.* **175**, 6789–6796.
Stewart, G. R., Robertson, B. D. & Young, D. B. (2003). *Nature Rev. Microbiol.* **2**, 97–105.
Stillman, T. J., Baker, P. J., Britton, K. L. & Rice, D. W. (1993). *J. Mol. Biol.* **234**, 1131–1139.
Usha, V., Jayaraman, R., Toro, J. C., Hoffner, S. E. & Das, K. S. (2002). *Can. J. Microbiol.* **48**, 7–13.
Vanhooke, J. L., Thoden, J. B., Brunhuber, N. M. W., Blanchard, J. S. & Holden, H. M. (1999). *Biochemistry*, **38**, 2326–2339.
Vancura, A., Vancurová, I., Volc, J., Jones, S. K., Flieger, M., Basarová, G. & Behal, V. (1989). *Eur. J. Biochem.* **15**, 221–227.
Vancurova, I., Vancura, A., Volc, J., Neuzil, J. & Behal, V. (1989). *J. Basic Microbiol.* **29**, 185–189.
Ward, M. J., Lew, H. & Zusman, D. R. (2000). *J. Bacteriol.* **182**, 546–550.